

# Lateral Control of Autonomous Vehicles with Sliding Angle Reconstruction

H. Fang<sup>1</sup>, R.X Fan<sup>1</sup>, B. Thuilot<sup>2</sup>, P. Martinet<sup>2</sup>

1. Pattern Recognition, Beijing Institute of Technology, Beijing 100081  
E-mail: fangh@bit.edu.cn

2. LASMEA, 4, av. des Landais, 63177 Aubiere Cedex, France  
E-mail: martinet@lasmea.univ-bpclermont.fr

**Abstract:** Lots of satisfactory results of high-precision lateral control have been reported with the assumption that vehicles move without sliding. But this assumption never comes true under real working conditions. More and more anti-sliding controllers have been designed which heavily relied on sophisticated control laws. Although the previous works can actually improve the guidance accuracy, the complexity and the rigorous requirements for the controller abilities make such controllers not very realistic for actual applications. In this paper a kinematic model is built which takes sliding effects into account by introducing two additional tire sliding angles. Based on this model an anti-sliding controller is designed. But unfortunately its efficiency completely depends on the estimation of the sliding parameters which cannot be directly measured by sensors. To overcome this problem an adaptive observer is designed using Lyapunov methods. With this observer, the cornering stiffness parameters instead of the sliding angles are estimated. The Lyapunov stability theory guarantees that the estimated value of the cornering stiffness would converge to its real value when the persistent excitation (PE) condition is satisfied. Consequently the sliding angles are reconstructed precisely. Simulation and experimental results show that the sliding effects can be compensated effectively by the combination of the anti-sliding controller and the sliding angle reconstruction.

**Key Words:** Lateral control, adaptive observer, autonomous vehicles

## 1 Introduction

Automatic steering control have been studied actively. Lots of results have been reported in recent years, but most of them focused their interests on control law design under the pure rolling condition which is never true for actual applications. Therefore the control results may deviate from its desired values. Sometimes stability and controllability of the autonomous systems may be broken because of unexpected sliding effects.

Until now there are very few papers dealing with sliding. [1] prevents cars from skidding by robust decoupling of car steering dynamics which is achieved by feedback of the integrated yaw rate into front wheel steering. [2] copes with the control of WMR (Wheeled Mobile Robot) not satisfying the ideal kinematic constraints by using slow manifold methods, but the parameters characterizing the sliding effects are assumed to be exactly known. In [3] a controller is designed based on the averaged model allowing the tracking errors to converge to a limit cycle near the origin. In [4] a general singular perturbation formulation is developed which leads to robust results for linearizing feedback laws ensuring trajectory tracking. But above two schemes only take into account sufficiently small sliding effects and they are too complicated for real-time practical implementation. In [5] [6] Variable Structure Control (VSC) is used to eliminate the harmful sliding effects when the bounds of

the sliding effects have been known. The trajectory tracking problem of mobile robots in the presence of sliding is solved in [7] by using discrete-time sliding mode control. But the controllers [5]-[7] counteract sliding effects **only** relying on high-gain controllers which is not realistic because of limited bandwidth and low level delay introduced by steering systems. In [8] sliding effects are rejected by re-scheming desired paths adaptively based on steady control errors which are mainly caused by modeled sliding effects. Moreover a robust adaptive controller is designed in [9] which compensates sliding by parameter adaptation and VSC. But the adaptive laws make the controller too complicated to be realized.

In the latest research paper [10] and [11], kinematic-based observers are designed with the concept of classical feedback control theories to estimate the sliding effects. The estimated sliding angles are integrated into the kinematic model which leads to an anti-sliding controller. But because only one GPS is available, a numerical derivation is necessary for state vector estimation.

In this paper side acceleration of vehicles is measured which provides necessary measurement data for sliding estimation. From these data the cornering stiffness which is only relevant to tire-ground characteristics is identified. Because it is rather difficult to identify a time-varying value especially when it cannot be modeled exactly, the advantage of the proposed scheme is that instead of the time-varying sliding effects, the cornering stiffness which is

---

This work was supported by Excellent young scholars Research Fund of Beijing Institute of Technology

nearly invariant is learned by an adaptive observer with high accuracy.

The main idea of this paper is that first the sliding effects are modeled by a function of the cornering stiffness, so the problem of sliding estimation is transformed into the problem of constant parameter identification which simplifies the tasks greatly. This paper is organized as follows, in section 2 the path following problem is described and a kinematic model considering sliding by two sliding angles is constructed. In section 3 an anti-sliding controller is designed based on chained system theories. In section 4 an adaptive observer is designed using Lyapunov analysis. In section 5 some comparative control results are presented to validate the proposed control laws.

## 2 Kinematic Model for Path Following Control

### 2.1 Notation and Problem Description

In this paper the vehicle is simplified into a bicycle model. The kinematic model is expressed with respect to the path in frame  $(M, \eta_t, \eta_n)$ , variables necessary in the kinematic model are denoted as follows:

- $C$  is the path to be followed.
- $O$  is the center of the vehicle virtual rear wheel.
- $M$  is the orthogonal projection of  $O$  on path  $C$ .
- $\eta_t$  is the tangent vector to the path at  $M$ .
- $\eta_n$  is the normal vector at  $M$ .
- $y$  is the lateral deviation between  $O$  and  $M$
- $s$  is the curvilinear coordinates (arc-length) of point  $M$  along the path from an initial position.
- $c(s)$  is the curvature of the path at point  $M$ .
- $\theta_d(s)$  is the orientation of the tangent to the path at point  $M$  with respect to the inertia frame.
- $\theta$  is the orientation of the vehicle centerline with respect to the inertia frame.
- $\tilde{\theta} = \theta - \theta_d$  is the orientation error.
- $l$  is the vehicle wheelbase.
- $v$  is the vehicle linear velocity.
- $\delta$  is the steering angle of the virtual front wheel

### 2.2 Kinematic Model

When autonomous vehicles move without sliding, the ideal kinematic model of the vehicles is (see [12] for details).

$$\begin{cases} \dot{s} = \frac{v \cos \tilde{\theta}}{1 - c(s)y} \\ \dot{y} = v \sin \tilde{\theta} \\ \dot{\tilde{\theta}} = v \left( \frac{\tan \delta}{l} - \frac{c(s) \cos \tilde{\theta}}{1 - c(s)y} \right) \end{cases} \quad (1)$$

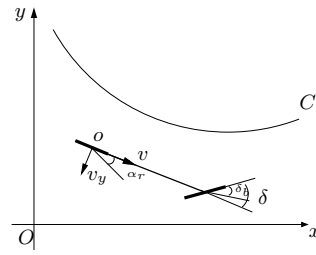


Figure 1: Notations of sliding effects

But when autonomous vehicles move on a steep slope or the ground is slippery, sliding occurs inevitably, (1) is no longer valid. The violation of the pure rolling constraints is described by introducing the rear sliding angle  $\alpha_r$  and the front sliding angle (also called Steering Angle Bias)  $\delta_b$  (figure 1). The kinematic constraints let  $\delta_b, \alpha_r$  be calculated by

$$\delta_b = \delta - \frac{l_f \gamma + v \tan \beta}{v} \quad (2)$$

$$\alpha_r = \frac{-l_r \gamma + v \tan \beta}{v} \quad (3)$$

where  $\beta$  is the sideslip angle and  $\gamma$  is the yaw rate at the mass center,  $l_f$  ( $l_r$ ) is the distance between the front (rear) wheel and the mass center.

Similar developing methods lead to a kinematic model with sliding

$$\begin{cases} \dot{s} = \frac{v \cos(\tilde{\theta} + \alpha_r)}{1 - c(s)y} \\ \dot{y} = v \sin(\tilde{\theta} + \alpha_r) \\ \dot{\tilde{\theta}} = v \left[ \cos \alpha_r \frac{\tan(\delta + \delta_b) - \tan \alpha_r}{l} - \frac{c(s) \cos(\tilde{\theta} + \alpha_r)}{1 - c(s)y} \right] \end{cases} \quad (4)$$

## 3 Anti-sliding controller design

### 3.1 Anti-sliding controller design based on chained form system

As presented in [12], in our previous work a path following controller has been designed by converting the model (1) into a chained system which allows using linear system theories to design nonlinear controllers (see [13]).

For a 3-D nonlinear system with two control inputs, the general chained system is written as

$$\text{derivation w.r.t } t \begin{cases} \dot{a}_1 = m_1 \\ \dot{a}_2 = a_3 m_1 \\ \dot{a}_3 = m_2 \end{cases} \quad (5)$$

Via state transformation as following

$$(a_1, a_2, a_3) = (s, y, (1 - c(s)y) \tan(\tilde{\theta} + \alpha_r)) \quad (6)$$

the kinematic model (4) can be transformed into the general chained system (5) in which

$$\begin{cases} m_1 = \frac{v \cos \tilde{\theta}_s}{\Gamma} \\ m_2 = \frac{d}{dt} \Gamma \tan \tilde{\theta}_s \end{cases} \quad (7)$$

where

$$\tilde{\theta}_s = \tilde{\theta} + \alpha_r \quad (8)$$

$$\Gamma = 1 - c(s)y \quad (9)$$

From (5)(6)(7), the expression of a single-input linear system can be obtained.

$$\text{derivation w.r.t } a_1 \begin{cases} a'_1 = 1 \\ a'_2 = a_3 \\ a'_3 = m_3 = \frac{m_2}{m_1} \end{cases} \quad (10)$$

where  $m_3$  is the virtual control input. As designed by [12] the virtual control input  $m_3$  is designed to be a PD-type controller

$$m_3 = -K_d a_3 - K_p a_2 \quad (K_p, K_d) \in R^{+2} \quad (11)$$

which leads to

$$a''_2 + K_d a'_2 + K_p a_2 = 0 \quad (12)$$

It is easy to prove that both the state  $a_2$  and  $a_3$  can converge to zero asymptotically by choosing  $K_d, K_p$ .

Through inverse conversion, the physical anti-sliding control law is obtained as

$$\begin{aligned} \delta(y, \tilde{\theta}) = \arctan \left( \frac{l}{\cos \alpha_r} \left[ \frac{\cos^3 \tilde{\theta}_s}{\Gamma^2} \left( \frac{dc(s)}{ds} y \tan \tilde{\theta}_s \right. \right. \right. \\ \left. \left. \left. - K_d a_3 - K_p a_2 + c(s)\Gamma \tan^2 \tilde{\theta}_s \right) \right. \right. \\ \left. \left. - \frac{1}{v} \frac{d\alpha_r}{dt} + \frac{c(s) \cos \tilde{\theta}_s}{\Gamma} \right] + \tan \alpha_r \right) - \delta_b \quad (13) \end{aligned}$$

Therefore the sliding effects may be completely compensated leading to accurate lateral control results when the sliding angles  $\alpha_r, \delta_b$  are exactly known.

Remark that when  $\alpha_r = \delta_b = 0$  which is to say that no sliding occurs, (13) is equal to the lateral controller with pure rolling assumption in [12].

### 3.2 Stability Analysis

(12) indicates both  $a_2$  and  $a_3$  converge to zero which means that

$$y = 0 \quad (14)$$

$$(1 - c(s)y) \tan(\tilde{\theta} + \alpha_r) = 0 \quad (15)$$

The singular condition  $y = \frac{1}{c(s)}$  is not considered in this paper, so it can be deduced that the system state  $\{y, \tilde{\theta}\}$  will converge to  $\{0, -\alpha_r\}$ . Consequently the vehicle would exactly follow the desired path in lateral direction, while its orientation error is still caused by the sliding effects. This ‘‘crab sliding’’ fact is consistent with the nature of the non-holonomic system which intends to control three states via two control inputs.

## 4 Sliding angle estimation by adaptive observer

In this section the unknown sliding angles will be reconstructed and the cornering stiffness will be identified by designing an adaptive observer. The main idea of this section is derived from [14]

### 4.1 2DOF bicycle model

The proposed observer is deduced from a 2DOF dynamic model of a vehicle which is simplified into a bicycle. By applying Newton’s laws and considering the linear lateral tire force model  $F_y = k_\alpha \alpha$ , the 2DOF dynamic model is defined as follows

$$\dot{x} = A_1 x + B_1 u \quad (16)$$

where

$$x = [\beta \quad \gamma \quad \theta]^T \quad (17)$$

$$A_1 = \begin{bmatrix} -\frac{2p_1}{mv} & -1 - \frac{2p_2}{mv^2} & 0 \\ -\frac{2p_2}{I_z} & -\frac{2p_3}{I_z v} & 0 \\ 0 & 1 & 0 \end{bmatrix} \quad (18)$$

$$B_1 = \begin{bmatrix} \frac{2k_f}{mv} & \frac{2k_r l_f}{I_z} & 0 \end{bmatrix} \quad (19)$$

$$I_z = ml_r l_f \quad (20)$$

$$p_1 = k_f + k_r \quad (21)$$

$$p_2 = k_f l_f - k_r l_r \quad (22)$$

$$p_3 = k_f l_f^2 + k_r l_r^2 \quad (23)$$

$u$  is the vector of the steering law.  $\beta, \gamma, \theta$  are defined as before.  $k_f$  ( $k_r$ ) is the constant representing the cornering stiffness of the front (rear) tire.

Moreover by differentiating (16) we have

$$\ddot{x} = A_1 \dot{x} + B_1 \dot{u} \quad (24)$$

### 4.2 State Equation of Side Acceleration

The side acceleration  $a_f, a_r$  at the front and rear axis can be written as

$$a_f = v(\dot{\beta} + \dot{\theta}) + l_f \dot{\gamma} \quad (25)$$

$$a_r = v(\dot{\beta} + \dot{\theta}) - l_r \dot{\gamma} \quad (26)$$

Defining a new state vector as

$$z = \begin{bmatrix} a_f \\ a_r \\ \gamma \end{bmatrix} = \begin{bmatrix} v & l_f & v \\ v & -l_r & v \\ 0 & 0 & 1 \end{bmatrix} \begin{bmatrix} \dot{\beta} \\ \dot{\gamma} \\ \dot{\theta} \end{bmatrix} = T \dot{x} \quad (27)$$

The derivative of (27) is

$$\dot{z} = T \ddot{x} = T A_1 T^{-1} z + T B_1 \dot{u} \quad (28)$$

Considering the first two row of (28) yields the following equation with  $a = (a_f, a_r)^T$  as the state vector

$$\dot{a} = A_2 (A_3 a + \tilde{u}) \quad (29)$$

where

$$A_2 = \begin{bmatrix} k_f & 0 \\ 0 & k_r \end{bmatrix} \quad (30)$$

$$A_3 = \begin{bmatrix} -\frac{2l}{l_r mv} & 0 \\ 0 & -\frac{2l}{l_f mv} \end{bmatrix} \quad (31)$$

$$\tilde{u} = \begin{bmatrix} \frac{2l}{l_r m}(\gamma + \dot{u}) \\ \frac{2l}{l_f m}\gamma \end{bmatrix} \quad (32)$$

Substitute (16) into (27) and regard  $a_r, a_f$  as known variables, the expression of  $\beta$  and  $\gamma$  can be obtained as following by solving the resulting equation

$$\begin{cases} \beta = \frac{l_r}{l}u - \frac{ml_r^2}{2k_f l^2}a_f - \frac{ml_f^2}{2k_r l^2}a_r \\ \gamma = \frac{v}{l}u - \frac{mv l_r}{2k_f l^2}a_f + \frac{mv l_f}{2k_r l^2}a_r \end{cases} \quad (33)$$

Remark that the side accelerations  $a_r, a_f$  can be measured by accelerometers and  $v$  can be obtained by GPS, so the unmeasurable sideslip angle  $\beta$  can be reconstructed by (33) when the cornering stiffness  $k_f, k_r$  are identified. Therefore the identification of  $k_f, k_r$  becomes a key issue for sliding angle estimation thanks to (2)(3).

#### 4.3 Side acceleration observation

To identify  $k_f, k_r$  the following side acceleration observer is used [14]

$$\dot{\hat{a}} = A_m \hat{a} + (\hat{A}_2 A_3 - A_m)a + \hat{A}_2 \tilde{u} \quad (34)$$

where  $\hat{A}_2 = \text{diag}(\hat{k}_f, \hat{k}_r)$  is the estimation of the unknown cornering stiffness to be identified.  $A_m = \text{diag}(p_{m1}, p_{m2})$  is a matrix satisfying Lyapunov equation.  $\hat{a} = [\hat{a}_f, \hat{a}_r]$  is the estimated value of the side acceleration.

Define the error of the acceleration estimation  $e = \hat{a} - a$ , the following equation holds because of (29) and (34)

$$\dot{e} = A_m e + \tilde{W}\phi \quad (35)$$

where

$$\tilde{W} = \begin{bmatrix} \frac{-2l}{l_r m v}a_f + \frac{2l}{l_r m}(\gamma + \dot{u}) & 0 \\ 0 & \frac{-2l}{l_f m v}a_r + \frac{2l}{l_f m}\gamma \end{bmatrix} \quad (36)$$

$$\phi = \begin{bmatrix} \hat{k}_f - k_f \\ \hat{k}_r - k_r \end{bmatrix} \quad (37)$$

The adaptive learning laws for  $\hat{k}_f, \hat{k}_r$  may be obtained by using Lyapunov stability theory. The Lyapunov function is defined as

$$V = e^T P_0 e + \phi^T Q_0 \phi \quad (38)$$

where  $P_0$  and  $Q_0$  are positive symmetric definite matrices and satisfy  $A_m^T P_0 + P_0 A_m = -Q_1 < 0$ , then the time derivative of  $V$  is

$$\dot{V} = -e^T Q_1 e + 2\phi^T (\tilde{W}^T P_0 e + Q_0 \dot{\phi}) \quad (39)$$

Let

$$\dot{\phi} = \begin{bmatrix} \dot{\hat{k}}_f \\ \dot{\hat{k}}_r \end{bmatrix} = -Q_0^{-1} \tilde{W}^T P_0 e \quad (40)$$

It can be obtained that

$$\dot{V} = -e^T Q_1 e \quad (41)$$

which guarantees the convergence of the acceleration estimation errors.

#### 4.4 Sliding angle reconstruction via identifying cornering stiffness

(41) leads to an accurate acceleration estimation. Furthermore the direct application of LaSalle invariance principle yields that  $\dot{e} \rightarrow 0$  and  $e \rightarrow 0$  which may consequently reach a conclusion that  $\tilde{W}\phi = 0$ .

The definition of  $\tilde{W}$  (36) guarantees that it is very easy to let  $\tilde{W}$  be a full rank matrix thanks to sufficient excitation of the steering law  $u$ . Therefore the result of  $\phi = 0$  can be deduced which leads to the results of  $\hat{k}_f = k_f$  and  $\hat{k}_r = k_r$ . So the cornering stiffness can be identified precisely by (40) if the operator provides sufficient excitation to the system.

Let  $Q_0$  be a identity matrix,  $P_0 = \text{diag}(p_f, p_r) > 0$ , the adaptive learning law can be represented by

$$\begin{bmatrix} \dot{\hat{k}}_f \\ \dot{\hat{k}}_r \end{bmatrix} = \begin{bmatrix} -w_f p_f (\hat{a}_f - a_f) \\ -w_r p_r (\hat{a}_r - a_r) \end{bmatrix} \quad (42)$$

where

$$w_f = \frac{-2l}{l_r m v}a_f + \frac{2l}{l_r m}(\gamma + \dot{u}) \quad (43)$$

$$w_r = \frac{-2l}{l_f m v}a_r + \frac{2l}{l_f m}\gamma \quad (44)$$

The key problem of identification of the cornering stiffness has been solved, then the vehicle sideslip angle  $\beta$  is estimated quite straightforward by

$$\hat{\beta} = \frac{l_r}{l}u - \frac{ml_r^2}{2\hat{k}_f l^2}a_f - \frac{ml_f^2}{2\hat{k}_r l^2}a_r \quad (45)$$

By substituting (45) into (2) and (3), the unknown sliding angles  $\delta_b, \alpha_r$  can be estimated which would make the anti-sliding controller (13) feasible and effective to moderate negative sliding effects.

### 5 Comparative Results

#### 5.1 Cornering stiffness identification

Identification of the cornering stiffness is most important to estimate the sliding angles. In order to validate the adaptive learning laws (42), a simulation is performed in which the the parameters are set as  $m=500\text{kg}$ ,  $l_f=1.1\text{m}$ ,  $l_r=1.3\text{m}$ ,  $k_f=25000\text{N/rad}$ ,  $k_r=32000\text{N/rad}$ .

A classical "U" path with perturbations is followed. In the simulations, the cornering stiffness parameters are initialized to zero, the gains used in (42) and (35) are set as  $p_f = 500000$ ,  $p_r = 2750000$ ,  $p_{m1} = -20$ ,  $p_{m2} = -3$ . The larger  $\|p_{m1}\|, \|p_{m2}\|$  are, the faster the acceleration estimation errors tend to zero, but the slower the estimation of  $\hat{k}_f, \hat{k}_r$  converges to the real values. On the other hand if  $p_f, p_r$  go too large, it may cause too much vibration of the estimation results of  $\hat{k}_f, \hat{k}_r$ , so in actual implementations these gains should be tuned gradually to make an optimal compromise between convergence rate and accuracy.

The estimation results of  $k_f, k_r$  are shown by figure 2 and 3 respectively. From these two figures it is known that although  $\hat{k}_f$  and  $\hat{k}_r$  have important initial errors, they can

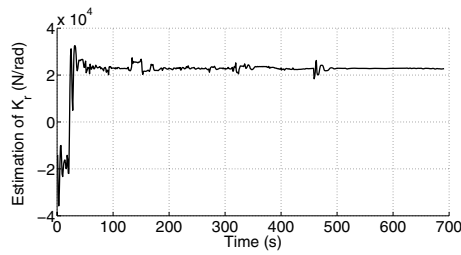


Figure 2: The estimation of  $k_f$

converge to their real values with high accuracy which provides necessary conditions for sideslip angle estimation. The sideslip angle  $\beta$  is estimated based on (45), the result is shown by figure 4. In this figure the solid line is the sideslip angle which is solved by dynamic model (16) providing the normal lab values of the sideslip angle. The dashed line depicts the estimated value of  $\beta$  from (45). Because the cornering stiffness has been identified with high accuracy, a good estimation of the sideslip angle may be obtained properly.

## 5.2 Experimental Results

The adaptive observer and sliding compensation system has been implemented and successfully tested on a combine-harvester. First the vehicle moved randomly on the ground which was slippery (such as a grass land or a slippery slope) for a while to identify the actual cornering stiffness. After the variation of the estimated values of the cornering stiffness was less than a defined threshold which meant that the estimated cornering stiffness has approached its real value, the vehicle began to follow a reference path. The front and rear sliding angles were computed on board and were fed into the anti-sliding controller (13).

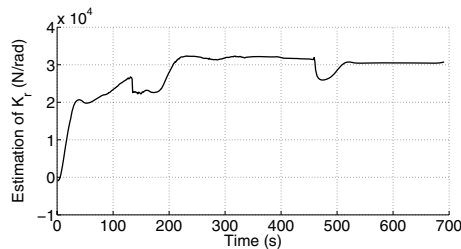


Figure 3: The estimation of  $k_r$

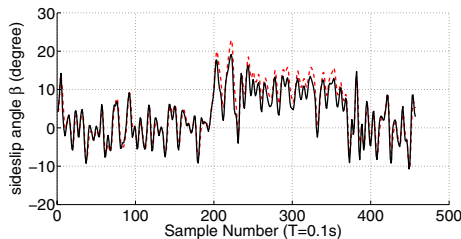


Figure 4: Estimation of side slip angle

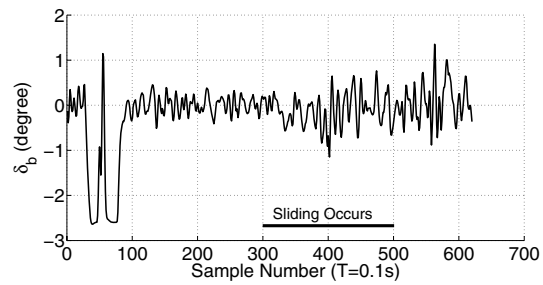


Figure 5: Front sliding angle estimation

Because the sliding angles could be reconstructed with high accuracy, the controller (13) moderated the negative sliding effects and improved the path following accuracy in great deal.

The experimental results are shown by figure 5-8. In figure 5 and 6, the results of the front/rear sliding angle estimation are displayed. Large sliding angles at the beginning of the test are recorded which are caused by initial adjustment of the vehicle's body attitude. Then the sliding angles are about zero which means that no obvious sliding occurs. When the vehicle follows a curve, the sliding angles increase which indicates that sliding would occur. Hence the lateral control results are deteriorated. In figure 7 the lateral deviations are demonstrated. The solid line is the lateral control result without sliding compensation. The dashed line is the result of the anti-sliding controller with sliding angle reconstruction. From those figures it is noticed that both experiments suffer from noticeable initial lateral errors caused by the initial orientation errors. As the vehicle follows the straight parts of the reference path, the lateral deviation obviously decreases vibrating within the range of 10cm which can meet the actual requirements. But when the vehicle steps into a circle, due to the slippery ground the maximum static-friction force of the tires cannot supply enough lateral forces to maintain the vehicle motion, tire sliding appears consequently resulting in significant lateral deviations (Solid line in figure 7). Thanks to the sliding angle estimation, the negative sliding effects can be moderated. So when the vehicle begins to follow a curve, although the low level delay may lead to important errors at the beginning and end of the curve tracing, the anti-sliding controller can still guarantee satisfying path following results with around 10cm accuracy (Dashed line) in spite of the sliding influences. The orientation errors are also displayed by figure 8. It is demonstrated that the controller with sliding compensation may improve the orientation control accuracy. But as analyzed by section (3.2), the orientation errors cannot be totally eliminated, so a crabwise motion is recorded. It is quite fit with the performance of the vehicle in actual experiments.

## 6 Conclusion

The problem of path following control of autonomous vehicles in presence of sliding is investigated in this paper. A kinematic model which considers sliding effects by two sliding angles is built. From this model, an anti-sliding

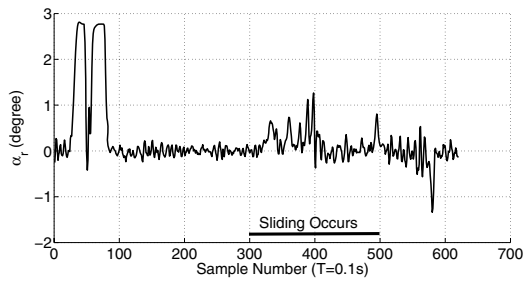


Figure 6: Rear sliding angle estimation

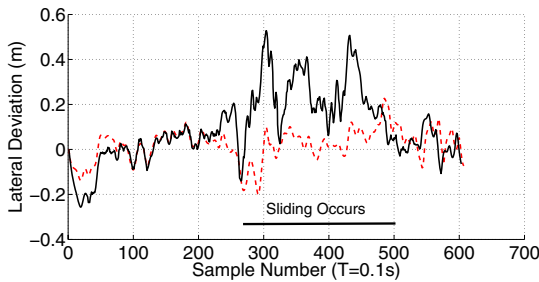


Figure 7: Lateral deviation of experimental results

controller is designed based on chained system theories. Since the sliding angles cannot be measured precisely, an adaptive observer is proposed based on Lyapunov analysis which leads to an accurate identification of the cornering stiffness. Simulation and experimental results show that by reconstructing the sliding angles online the sliding effects can be properly moderated. The conclusion of this paper is also remarkable for general vehicles.

## REFERENCES

- [1] J. Ackermann, "Robust control prevents car skidding". *IEEE Control Systems Magazine*, pp: 23-31, June,1997.
- [2] I. Motte, H. Campion, "Control of sliding mobile robots : a slow manifold approach", MNTS, 2000.
- [3] W. Leroquais, B. D'Andrea-Novet, "Vibrational control of wheeled mobile robots not satisfying ideal velocity constraints: the unicycle case", *European Control Conference*. July 1-4, Brussels, 1997.
- [4] B. D'Andrea-Novet, G. Campion and G. Bastin, "Control of wheeled mobile robots not satisfying ideal constraints:

- a singular perturbation approach", *International Journal of Robust Nonlinear Control*, 5: 243-267, 1995.
- [5] Y. L. Zhang, J. H. Chung, S. A. Velinsky, "Variable structure control of a differentially steered wheeled mobile robot", *Journal of intelligent and Robotic Systems*. 36: 301-314, 2003.
- [6] H. Fang, R. Lenain, B. Thuilot, P. Martinet, "Sliding Mode Control of Automatic Guidance of Farm Vehicles in the Presence of Sliding". *The 4th International Symposium on Robotics and Automation*, Queretaro, Mexico August 25-27. pp. 582-587, 2004.
- [7] M. L. Corradini and G. Orlando, "Experimental testing of a discrete-time sliding mode controller for trajectory tracking of a wheeled mobile robot in the presence of skidding effects". *Journal of robotic systems*, 19(4), 177-188, 2002.
- [8] Lenain R. Thuilot B. Cariou C, Martinet P. , "Adaptive control for car like vehicles guidance relying on RTK GPS: rejection of sliding effects in agricultural applications". *In Proc. of the intern. Conf. On Robotics and Automation*, Taipei, Sept, pp. 115-120, 2003.
- [9] H. Fang, R. Lenain, B. Thuilot, P. Martinet, "Robust Adaptive Control of Automatic Guidance of Farm Vehicles in the Presence of Sliding", *IEEE International Conference on Robotics and Automation*, Barcelona, April, 18-22, pp. 3113-3118, 2005.
- [10] Lenain R. Thuilot B. Cariou C, Martinet P, "Sideslip angles observer for vehicle guidance in sliding conditions: Application to agricultural path tracking tasks", *In Proc. of the intern. Conf. On Robotics and Automation*, Orlando, Florida, May , pp. 3183-3188, 2006.
- [11] Lenain R. Thuilot B. Cariou C, Martinet P. , "Mobile robot control in presence of sliding: Application to agricultural vehicle path tracking", *In Proc. of the 45th IEEE Conference on Decision & Control*, San Diego, CA, USA, December 13-15, pp. 6004-6009, 2006.
- [12] Thuilot B, Cariou C, Martinet P, and Berducat M, "Automatic guidance of a farm tractor relying on a single CP-DGPS", *Autonomous robots* , 13(1): 87-104,2002
- [13] Samson, C, Control of chained systems, "Application to path following and time-varying point stabilization of mobile robot", *IEEE Trans, on Automatic Control*, 39(12): pp. 2411-2425, 1995.
- [14] T. Hiraoka, H. Kumamoto, O. Nishihara and K. Tenmoku , "Cooperative Steering System Based on Vehicle Sideslip Angle Estimation from Side Acceleration Data at Percussion Centers", *Proc. of IEEE International Vehicle Electronics Conference 2001(IVEC2001)*, pp.79-84 (2001.9)

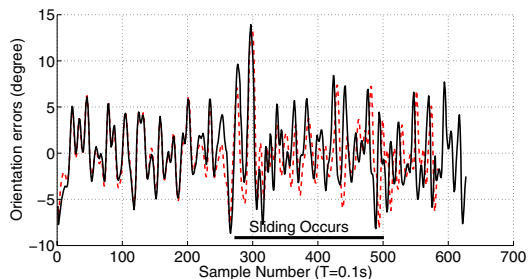


Figure 8: Orientation error of experimental results